

## Atomic-Scale Characterization of the Reduction of $\alpha$ -Fe<sub>2</sub>O<sub>3</sub> Nanowires

Wenhui Zhu<sup>1</sup>, Jonathan P Winterstein<sup>2</sup>, Renu Sharma<sup>2</sup> and Guangwen Zhou<sup>1</sup>

<sup>1</sup> Department of Mechanical Engineering & Multidisciplinary Program in Materials Science and Engineering, State University of New York, Binghamton, NY 13902, USA

<sup>2</sup> Center for Nanoscale Science and Technology, National Institute of Standards and Technology, Gaithersburg, MD 20899, USA

Reduction of metal oxides is a reaction of removing lattice oxygen and plays an role in producing active materials for a variety of applications ranging from catalysis to electronic devices [1]. The reduction of iron oxides has been investigated intensively because of its vital role in heterogeneous catalysis. The variable valence states of Fe cause a rather complicated Fe-O phase diagram, leading to the possibility of multiple phases being formed during redox reactions. It has, therefore, been a longstanding challenge in understanding the reduction mechanism of Fe<sub>2</sub>O<sub>3</sub>. Here, we present observations of an iron oxide superlattice structure resulting from oxygen vacancy ordering and stacking fault formation as well as the phase transformation pathway during the reduction of  $\alpha$ -Fe<sub>2</sub>O<sub>3</sub> nanowires

The  $\alpha$ -Fe<sub>2</sub>O<sub>3</sub> nanowires were prepared by the thermal oxidation of pure iron [2]. The reduction was conducted in a vacuum chamber at T = 500 °C with the pressure of H<sub>2</sub> gas (99.999% purity) at 270 Pa. The morphologies of the nanowires both before and after the H<sub>2</sub> reduction were examined using a scanning electron microscope (SEM). The crystal structure and valence state of the nanowires were characterized by TEM imaging, diffraction, and electron energy-loss spectroscopy using an aberration-corrected TEM operated at 300 kV.

Fig. 1 shows SEM images of the nanowires before and after the reduction reaction. It can be seen that the as-prepared nanowires have a smooth surface morphology while the reduced nanowires show the formation of bulges on the surface. Fig. 2 (a) illustrates a bright-field TEM image of a single reduced nanowire with the presence of bulges on the surface. Fig. 2 (b) presents a HRTEM image at relative low magnification of the parent nanowire as marked with the red square in Fig. 2 (a). The upper-right inset in Fig. 2 (b) is an optical diffractogram of the HRTEM image, which shows the presence of superlattice diffraction spots in addition of the fundamental reflections associated with the  $\alpha$ -Fe<sub>2</sub>O<sub>3</sub> structure of the parent nanowire. The lower-right inset in Fig. 2 (b) is simulated diffraction pattern using the  $\alpha$ -Fe<sub>2</sub>O<sub>3</sub> structure with the removal of oxygen atoms (i.e., the ordering of oxygen vacancies) of every 10<sup>th</sup> {3 $\bar{3}$ 00} plane. Fig. 2 (c) illustrates the formation of another type of defects, i.e., stacking faults, with the shifting of atomic planes, forming the banded structure in the parent region of the reduced nanowire. There have been several reports suggesting that the formation of the modulated structure in  $\alpha$ -Fe<sub>2</sub>O<sub>3</sub> is caused either by oxygen-vacancy ordering [3] or by stacking fault formation [4]. Here we find that both oxygen-vacancy ordering and stacking faults appear during the reduction process.

In addition to the formation of the modulated structure by ordering of oxygen vacancies or stacking faults, phase transitions are also observed in the reduced nanowires. Fig. 3 (a) shows a TEM image of a reduced nanowire. The diffraction pattern (inset in Fig. 3(a)) shows that both the parent and the bulge area have a cubic structure, which can be indexed either as  $\gamma$ -Fe<sub>2</sub>O<sub>3</sub> (space group: *P*4<sub>1</sub>32; nearly cubic with a small tetragonal distortion) or Fe<sub>3</sub>O<sub>4</sub> (space group: *Fd* $\bar{3}m$ ) due to their close lattice constants. Electron energy loss spectroscopy (EELS) was used to further distinguish the two structures. Fig. 3 (b)

shows the Fe L edge. The  $L_3/L_2$  ratio of the parent nanowire is  $\sim 5.0$ , higher than that of the bulge area ( $\sim 4.5$ ), indicating their different oxidation states, i.e., the parent nanowire is  $\gamma\text{-Fe}_2\text{O}_3$  while the bulge area is  $\text{Fe}_3\text{O}_4$ . Due to the similar lattice constants of the two phases, their interface is coherent and the  $\text{Fe}_3\text{O}_4$  bulge forms epitaxially with the  $\gamma\text{-Fe}_2\text{O}_3$  nanowire (Fig. 3 (c)), where the  $\gamma\text{-Fe}_2\text{O}_3$  phase is formed by the conversion reaction of the initial  $\alpha\text{-Fe}_2\text{O}_3$  nanowire. Fig. 3(d) is a simulated HRTEM image of the  $\gamma\text{-Fe}_2\text{O}_3/\text{Fe}_3\text{O}_4$  interface, which matches well with the experimental one shown in Fig. 3(c). In conclusion, TEM analysis indicates the reduction process involves the formation of a superlattice caused by both oxygen-vacancy ordering and stacking faults and a topotactic reaction from  $\gamma\text{-Fe}_2\text{O}_3$  to  $\text{Fe}_3\text{O}_4$ .

## References:

- [1] Luo, W., et al., *Journal of Physics D: Applied Physics*, 2007. **40**(4): p. 1091.
- [2] Yuan, L., et al., *Nanoscale*, 2013. **5**(16): p. 7581-7588.
- [3] Chen, Z., et al., *Chemistry of Materials*, 2008. **20**(9): p. 3224-3228.
- [4] Cai, R., *Chinese Physics B*, 2013. **22**(10): p. 107401.

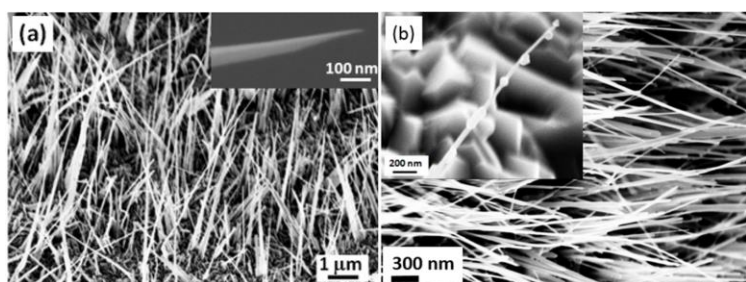


**Figure 1.** (a) SEM image of the as-prepared  $\alpha\text{-Fe}_2\text{O}_3$  nanowires, with the inset showing the smooth surface and tapered tip of the nanowires [2], (b) SEM image of the reduced nanowires with the inset showing bulge formation on the parent nanowires.

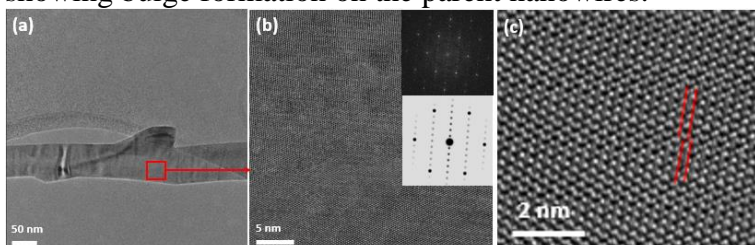


**Figure 2.** (a) a single  $\alpha\text{-Fe}_2\text{O}_3$  nanowire after the  $\text{H}_2$  reduction, (b) HRTEM image showing the presence of superlattice due to oxygen-vacancy ordering, the insets are the experimental and simulated diffractograms, and (c) HRTEM showing the presence of stacking faults (image filtered to reduce noise).

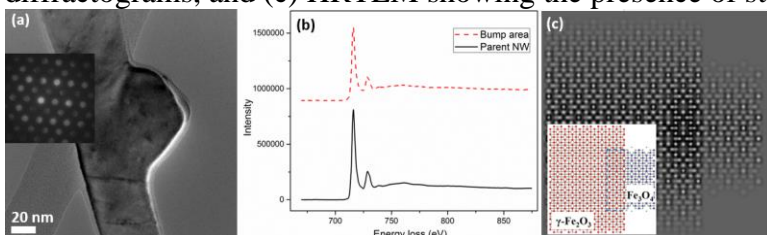


**Figure 3.** (a) Iron oxide Nanowires with bump along the parent nanowire, the inset shows the [110] zone-axis diffraction pattern from both the parent nanowire and bulge area, (b) EELS of the two areas with different  $L_3/L_2$  ratios of Fe L edge, indicating that the parent nanowire is  $\gamma\text{-Fe}_2\text{O}_3$  and the bump area is  $\text{Fe}_3\text{O}_4$ , (c) HRTEM image showing the  $\gamma\text{-Fe}_2\text{O}_3/\text{Fe}_3\text{O}_4$  interface area, (d) The simulated HRTEM of  $\gamma\text{-Fe}_2\text{O}_3$  and  $\text{Fe}_3\text{O}_4$ , with the inset of the structure model, showing a coherent interface.